ISSN 2072-5981
doi: 10.26907/mrsej

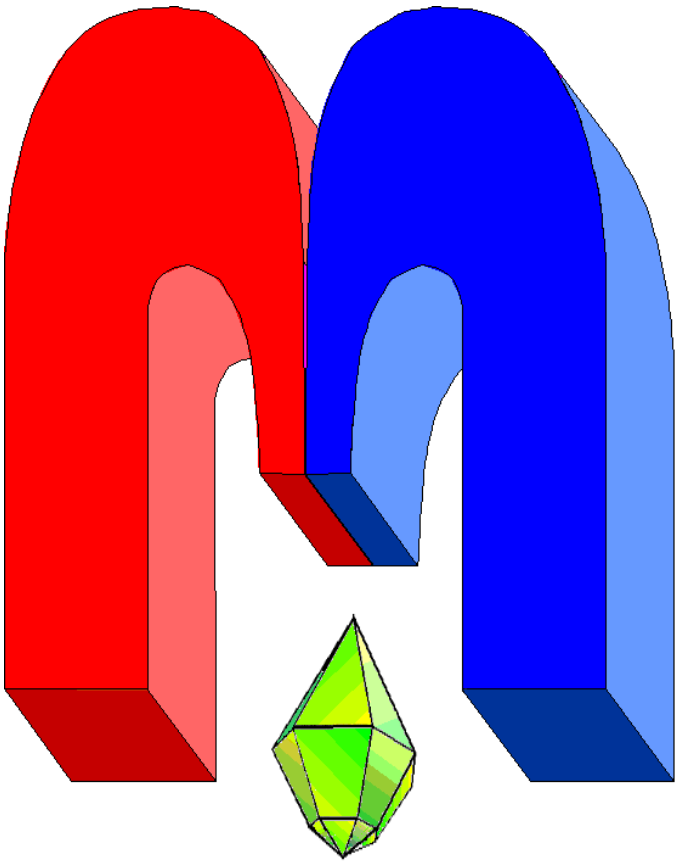

Magnetic Resonance in Solids

Electronic Journal

Volume 21
Issue 6
Article No 19601
1-11 pages
2019
doi: **10.26907/mrsej-19601**

http://mrsej.kpfu.ru
http://mrsej.ksu.ru

Established and published by Kazan University
Endorsed by International Society of Magnetic Resonance (ISMAR)
Registered by Russian Federation Committee on Press (#015140), August 2, 1996
First Issue appeared on July 25, 1997

© Kazan Federal University (KFU)*

"***Magnetic Resonance in Solids. Electronic Journal***" (**MRS*ej***) is a peer-reviewed, all electronic journal, publishing articles which meet the highest standards of scientific quality in the field of basic research of a magnetic resonance in solids and related phenomena.

Indexed and abstracted by
Web of Science (*ESCI*, Clarivate Analytics, from 2015), *Scopus* (Elsevier, from 2012), *RusIndexSC* (*eLibrary*, from 2006), *Google Scholar*, *DOAJ*, *ROAD*, *CyberLeninka* (from 2006), *SCImago Journal & Country Rank*, etc.

Editor-in-Chief
Boris **Kochelaev** (KFU, Kazan)

Honorary Editors
Jean **Jeener** (Universite Libre de Bruxelles, Brussels)
Raymond **Orbach** (University of California, Riverside)

Executive Editor
Yurii **Proshin** (KFU, Kazan)
mrsej@kpfu.ru

Editors
Vadim **Atsarkin** (Institute of Radio Engineering and Electronics, Moscow)
Yurij **Bunkov** (CNRS, Grenoble)
Mikhail **Eremin** (KFU, Kazan)
David **Fushman** (University of Maryland, College Park)
Hugo **Keller** (University of Zürich, Zürich)
Yoshio **Kitaoka** (Osaka University, Osaka)
Boris **Malkin** (KFU, Kazan)
Alexander **Shengelaya** (Tbilisi State University, Tbilisi)
Jörg **Sichelschmidt** (Max Planck Institute for Chemical Physics of Solids, Dresden)
Haruhiko **Suzuki** (Kanazawa University, Kanazava)
Murat **Tagirov** (KFU, Kazan)
Dmitrii **Tayurskii** (KFU, Kazan)
Valentine **Zhikharev** (KNRTU, Kazan)

This work is licensed under a Creative Commons Attribution-ShareAlike 4.0 International License.

This is an open access journal which means that all content is freely available without charge to the user or his/her institution. This is in accordance with the BOAI definition of open access.

Technical Editor
Maxim **Avdeev** (KFU, Kazan)

* In Kazan University the Electron Paramagnetic Resonance (EPR) was discovered by Zavoisky E.K. in 1944.

EPR spectra and magnetization of XY-type rare-earth ions in pyrochlores $Y_2Ti_2O_7$:RE^{3+} (RE=Yb, Er)

R.G. Batulin, M.A. Cherosov, I.F. Gilmutdinov, A.G. Kiiamov,
V.V. Klekovkina*, B.Z. Malkin, A.A. Rodionov, R.V. Yusupov

Kazan Federal University, Kremlevskaya 18, Kazan 420008, Russia

**E-mail: Vera.Klekovkina@kpfu.ru*

(Received November 24, 2019; revised December 8, 2019;
accepted December 9, 2019; published December 10, 2019)

The results of studies of $Y_2Ti_2O_7$ single crystals doped with Er^{3+} and Yb^{3+} ions by means of electron paramagnetic resonance (EPR) and dc-magnetometry are reported. EPR signals of the trigonal centers with the characteristic hyperfine structure of Er^{3+} or Yb^{3+} ions were observed. Field dependences of magnetization of single crystals for magnetic fields directed along the crystallographic axes and temperature dependences of magnetic susceptibilities were measured. Spin Hamiltonian parameters (g-factors and parameters of the hyperfine interaction) for Er^{3+} and Yb^{3+} ions were obtained from analysis of experimental data. The registered EPR spectra and magnetization curves were successfully reproduced by simulations in framework of the crystal-field approach, in particular, with an account for hybridization of ground $4f^{13}$ configuration of Yb^{3+} ions with the charge transfer states.

PACS: 71.70.Ch, 75.10.Dg, 76.30.Kg, 71.70.Ej.

Keywords: rare-earth pyrochlores, electron paramagnetic resonance, magnetization, magnetic susceptibility, crystal field, g-factors, hyperfine interaction.

1. Introduction

Extensive experimental and theoretical studies of magnetic structures and excitations in the so called XY pyrochlores containing rare-earth (RE) Er^{3+} and Yb^{3+} ions with the easy-plane magnetic anisotropy have been carried out over the last twenty years ([1–3] and references therein). A diversity of magnetic phases in the concentrated materials $Yb_2M_2O_7$ and $Er_2M_2O_7$ (M=Ge^{4+}, Ti^{4+}, Pt^{4+}, Sn^{4+}) was revealed at low temperatures (noncoplanar ψ_2 or coplanar ψ_3 antiferromagnetic order [4–7], antiferromagnetic phase of Palmer-Chalker [8,9], splayed ferromagnetic order [10–14]).

RE ions in pyrochlore (space group $Fd\bar{3}m$) crystal lattice occupy 16d Wyckoff positions with the local trigonal symmetry D_{3d}. Four magnetically non-equivalent RE sublattices form a corner-sharing tetrahedral network, the basis vectors of RE^{3+} ions in the unit cell in the crystallographic system of coordinates with the origin at the center of a corresponding tetrahedron are as follows: $\mathbf{r}_1 = (1,1,1)/8$, $\mathbf{r}_2 = (-1,-1,1)/8$, $\mathbf{r}_3 = (-1,1,-1)/8$, $\mathbf{r}_4 = (1,-1,-1)/8$ in units of the lattice constant a. The first coordination shell of RE ions contains eight oxygen ions which form strongly distorted cubic polyhedron with the two nearest neighbor oxygen ions at one of the four crystallographic [111] axes. Specific magnetic properties of different RE pyrochlores are determined, first of all, by the single RE ion magnetic characteristics and the energy spectrum in the trigonal crystal field (CF).

The wave functions of the ground Kramers doublet of Er^{3+} and Yb^{3+} ions in the trigonal CF transform accordingly to the irreducible representations Γ_4 or Γ_{56} of the D_{3d} point symmetry group. Note that magnetic properties of these states are substantially different, in particular, the so called dipole-octupole doublets Γ_{56} are split only by the magnetic field parallel to the trigonal symmetry axis (the transversal g-factor $g_\perp = 0$) while both the longitudinal ($g_\parallel$) and

the transversal g-factors of the Γ_4 doublets are non-zero.

The CF splittings of the electronic $4f^N$ – multiplets and spectroscopic g-factors of Er^{3+} ($N = 11$) and Yb^{3+} ($N = 13$) ions in dilute and concentrated pyrochlores were extensively studied earlier. The g-factors of the ground state of Yb^{3+} ions were determined from ^{170}Yb Mössbauer absorption measurements in $Y_2Ti_2O_7$:Yb^{3+} (1 at.%) sample enriched with the ^{170}Yb isotope in Ref. [15], but g-factors of Er^{3+} ions were estimated only from calculations based on CF parameters which had been used for simulations of dc-magnetic susceptibility of $Er_2Ti_2O_7$ [27]. Some CF energies of Yb^{3+} ions in $Y_2Ti_2O_7$:Yb^{3+} and $Yb_2Ti_2O_7$ were measured by means of optical spectroscopy [17]. CF excitations corresponding to transitions between sublevels of the ground multiplets of Yb^{3+} and Er^{3+} in $Yb_2Ti_2O_7$ and $Er_2M_2O_7$ (M=Ge, Ti, Sn, Pt, Ru) were studied by means of inelastic neutron scattering in Refs. [18, 19] and [20, 21], respectively.

The CF approach serves as basis for construction of theoretical models of interactions between RE ions and a crystal lattice and for understanding magnetic properties of concentrated RE compounds. A number of CF parameter sets for Er^{3+} and Yb^{3+} in the pyrochlores with different chemical compositions were proposed in literature (see [1,22,23] and references therein). However, the comment written 18 years ago [15], namely, "All are inappropriate as each corresponds to a crystal level scheme and to the ground state wave functions which are not compatible with the experimental data", is actual nowadays as well. Determination of the physically consistent CF parameters describing both the measured g-factors and CF energies remains a topical problem.

In recent work [24], stimulated by the increasing interest to the unconventional magnetic properties of geometrically frustrated RE pyrochlores, we presented the measured electron paramagnetic resonance (EPR) and site-selective emission and excitation optical spectra of $Y_2Ti_2O_7$ single crystals doped with Er^{3+} and Yb^{3+} ions (0.5 at.%). The CF parameters were calculated in the framework of the semi-phenomenological exchange charge model and then corrected to fit the experimental data. The main goal of present work is to obtain additional information about electronic structures of pyrochlores containing XY-type RE ions (Er^{3+} or Yb^{3+}).

We present low-temperature magnetic field dependences of magnetization and temperature dependences of the bulk dc-susceptibility of $Y_2Ti_2O_7$:Yb^{3+} and $Y_2Ti_2O_7$:Er^{3+} (0.5 at.%) single crystals. The shape and the hyperfine structure of EPR signals presented in [24] and magnetization curves are analyzed by making use of the corresponding sets of CF parameters.

2. Experimental details and results

The measurements of the magnetization $M(\mathbf{B}, T)$ parallel to the external magnetic field $\mathbf{B}$ with magnetic fields in the range of 0-9 T applied along the crystallographic axes [100], [111] and [110] were performed using a vibrating sample magnetometer option of the PPMS-9 system (Quantum Design) on $Y_2Ti_2O_7$:Yb^{3+} and $Y_2Ti_2O_7$:Er^{3+} single crystals with the content of 0.5 at.% of impurity ions grown by the optical floating-zone method [25]. The details of the single crystal growths were described in [24]. The pyrochlore structure of the samples was confirmed by X-ray diffraction measurements.

The obtained magnetic field dependences of the magnetization at the temperature T of 2 K are shown in Figure 1. The experimental data in Figure 1 are corrected by accounting for diamagnetic contributions [26] into the measured magnetization which are substantial in case of strongly diluted samples.

For weak magnetic fields, $B < 1$ T, the magnetization $M(\mathbf{B}, T)$ is practically isotropic, as

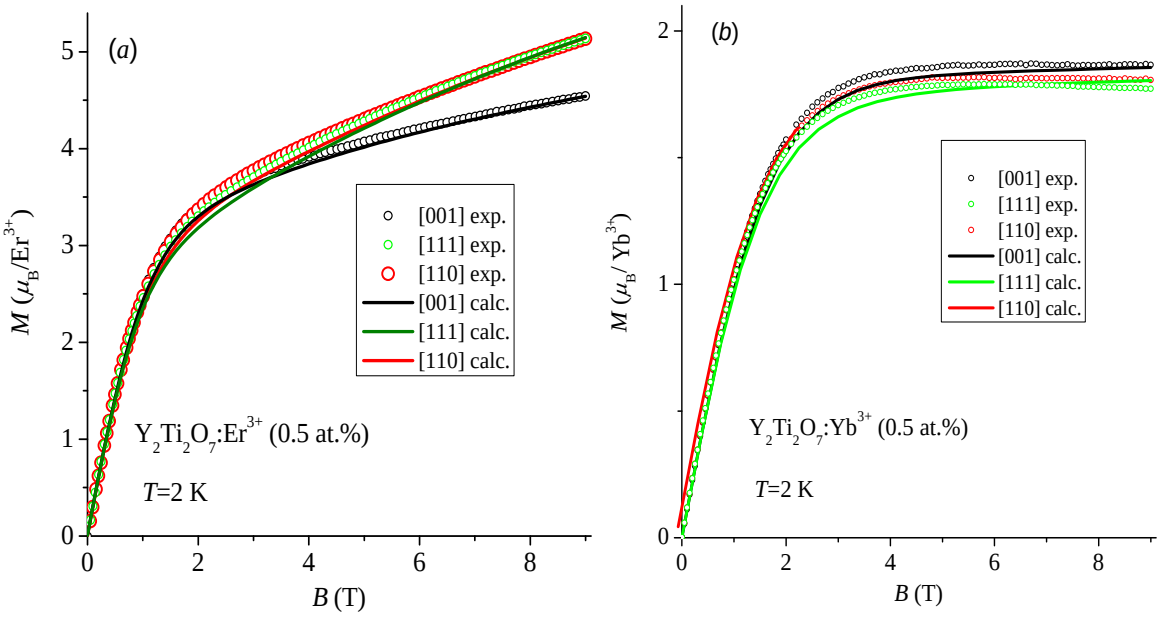

Figure 1. Measured (symbols) and calculated (solid curves) field dependences of the magnetization of $Y_2Ti_2O_7$:Er^{3+} (a) and $Y_2Ti_2O_7$:Yb^{3+} (b) single crystal for magnetic fields **B** directed along the crystallographic axes at temperature T=2 K.

one may expect in case of global cubic symmetry of the studied systems. The temperature dependences of the static magnetic susceptibility $\chi(T) = M(B,T)/B$ of $Y_2Ti_2O_7$:Yb^{3+} and $Y_2Ti_2O_7$:Er^{3+} single crystals measured in the magnetic fields B=0.4 T and 0.3 T, respectively, are presented in Figure 2.

The measured susceptibility curves can be satisfactorily approximated by the Curie law, $\chi(T) = C/T$ with the Curie constant $C = 2cN_A g^2 J(J+1)\mu_B^2/3k_B$ at elevated temperatures and $C = 2cN_A(g_{||}^2 + 2g_{\perp}^2)\mu_B^2/3k_B$ at low temperatures (here c is the concentration of RE ions, N_A is the Avogadro number, μ_B is the Bohr magneton, k_B is the Boltzmann constant, g is the Lande factor of the ground multiplet with the total angular moment J, $g_{||}$ and $g_{\perp}$ are the g-factors of the ground Kramers doublet determined from the EPR spectra (see below)). As the magnetic field increases, a noticeable dependence of the magnetization on the field direction appears due to mixing of wave functions of the ground and excited CF levels by the Zeeman interaction (see Figure 1). Of particular interest for justification of the CF parameter sets is the difference in the relative shifts of magnetization curves of Er^{3+} and Yb^{3+} ions in magnetic fields along the tetragonal [001] axis, in this case the observed magnetization in strong magnetic fields has maximum values for the Yb^{3+} ions but minimum values for the Er^{3+} ions. The gaps of $\sim 600\,cm^{-1}$ and $\sim 50\,cm^{-1}$ between the ground Γ_4 doublet and the first excited state of Yb^{3+} and Er^{3+} ions [24], respectively, differ by more than an order of magnitude, and, in agreement with the nonlinear mechanism of the single-ion magnetic anisotropy in cubic paramagnetic centers, it is remarkably stronger in $Y_2Ti_2O_7$:Er^{3+} than in $Y_2Ti_2O_7$:Yb^{3+} single crystals. The EPR spectra were measured with the commercial Bruker ESP300 X-band spectrometer in static magnetic fields up to 550 mT. The registered spectra of the $Y_2Ti_2O_7$:Yb^{3+} and $Y_2Ti_2O_7$:Er^{3+} (0.5 at.%) single crystals with the magnetic fields directed along the crystallographic axes are shown in Figures 3 and 4, respectively. Using the measured resonant magnetic fields of even isotopes, we found the corresponding effective g-factors.

The spectra measured with the magnetic field **B** directed along the tetragonal [001] axis con-

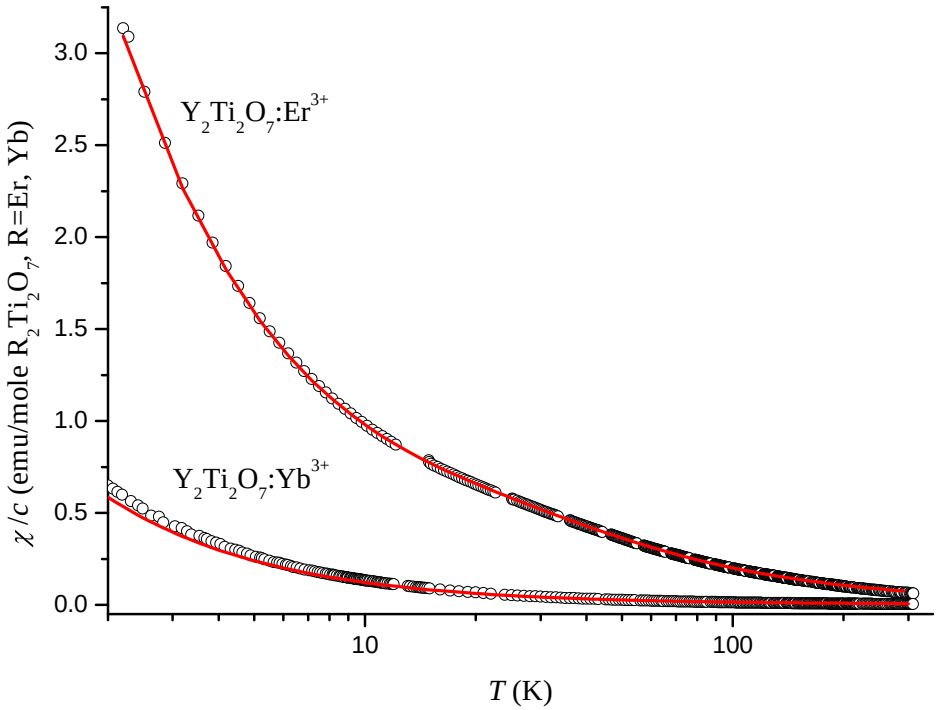

Figure 2. Measured (symbols) and calculated (solid curves) temperature dependences of the renormalized dc-susceptibilities $\chi[Y_{2-2c}RE_{2c}Ti_2O_7]/c$ (RE=Er, Yb, c=0.005).

tain one intense line corresponding to the g-factor $g_{[001]} = \sqrt{g_\parallel^2/3 + 2g_\perp^2/3}$ of four magnetically equivalent paramagnetic centers (here and below $g_\parallel$ and $g_\perp$ are g-factors in local coordinate frames with the Z-axis along the trigonal symmetry axis of the corresponding center).

If the external magnetic field is parallel to a trigonal [111] axis, there are two magnetically non-equivalent centers of RE^{3+} ions: one site whose local anisotropy axis is parallel to the static magnetic field B and three sites have their local anisotropy axis at $\sim$ 109.5 degrees from the vector **B**.

In the magnetic field applied along the two-fold rhombic [110] axis, there are also two magnetically non-equivalent centers: two so-called α-sites (the magnetic field is declined from the local trigonal axis by the angle of $\sim$ 35.3 degrees) and two β-sites (the field is perpendicular to the local trigonal axis). Therefore in cases of static magnetic field directed along trigonal or rhombic axes, two EPR lines with different intensities corresponding to the g-factors $g^{(1)}_{[111]} = g_\parallel$, $g^{(2)}_{[111]} = \sqrt{g_\parallel^2/9 + 8g_\perp^2/9}$, $g^{(1)}_{[110]} = \sqrt{2g_\parallel^2/3 + g_\perp^2/3}$, $g^{(2)}_{[110]} = g_\perp$ are observed. The sum of squared g-factors over four ion sites in the unit cell for each direction of the magnetic field that determines the linear magnetic susceptibility is a constant.

Along with the most intensive signals from even isotopes, the spectra contain weaker components of the hyperfine structure originating from odd isotopes (^{167}Er with the nuclear spin $I = 7/2$ and natural abundance of 22.9 %, ^{171}Yb (14.3 %) and ^{173}Yb (16.2 %) with $I = 1/2$ and $I = 5/2$, respectively). The measured values of the g-factors, $g_\parallel$ and $g_\perp$, and the hyperfine structure parameters for odd isotopes are presented in Table 2. We note that the g-factors of Er^{3+} ions in the concentrated Er-pyrochlope $Er_2Ti_2O_7$ $g_\parallel = 2.6$ from Ref. [27] (polarized neutron diffraction measurements) and $g_\perp = 2.7$ [28] (low-temperature EPR transmission-type spectroscopy) are rather far from our values.

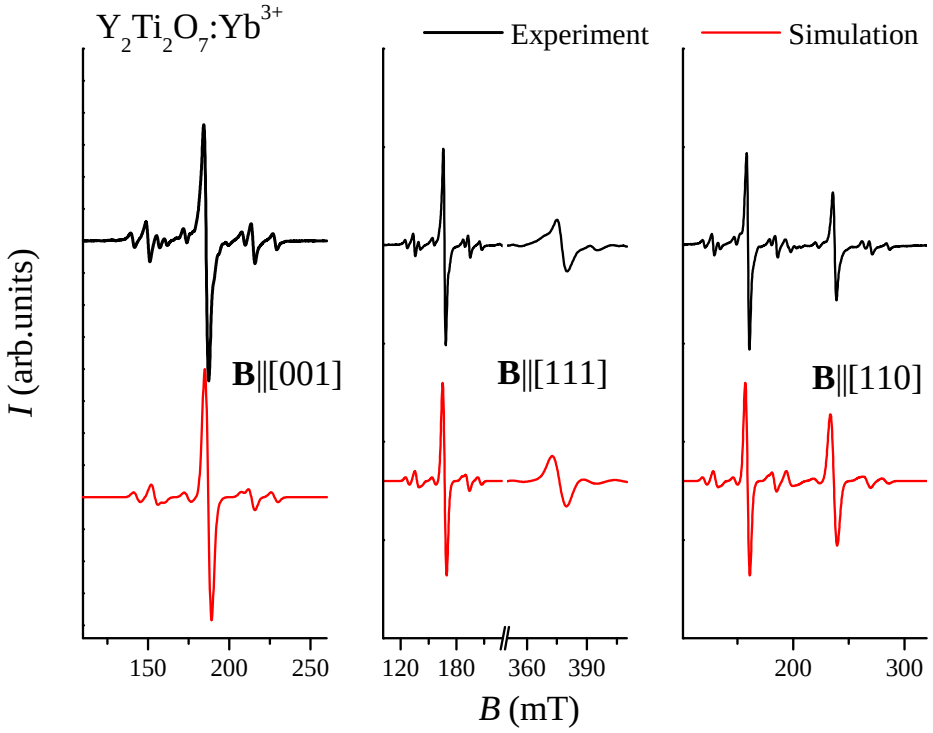

Figure 3. EPR spectra of the $Y_2Ti_2O_7$:Yb^{3+} (0.5 at.%) single-crystal for three orientations of the magnetic field **B** ($\nu = 9.41553$ GHz, $T = 15$ K). Experimental data and the results of simulations are shown by solid black and red lines, respectively. Linewidths of the spectral components of the simulated spectra had the values of $\sigma = 0.105$ GHz for **B** ∥ [001], 0.12 GHz for **B** ∥ [110], and $\sigma_1 = 0.09$ GHz and $\sigma_2 = \sigma_3 = \sigma_4 = 0.12$ GHz for **B** ∥ [111].

3. Discussion

In order to simulate the EPR spectra, magnetization and susceptibility data, we considered the following Hamiltonian of the Er^{3+} ion

$$H = H_{\rm FI} + H_{\rm CF} + H_{\rm Z} + H_{\rm HF}. \tag{1}$$

Here $H_{\rm FI}$ is the free ion standard parameterized Hamiltonian [29] that operates in the total space of 364 states of the electronic $4f^{11}$ configuration. $H_{\rm CF}$ is the CF energy of 4f electrons, $H_{\rm Z}$ is the electronic Zeeman energy, and $H_{\rm HF}$ corresponds to the hyperfine interaction. The free-ion Hamiltonian is written as follows

$$\begin{aligned} H_{\rm FI} = \zeta \sum_i \mathbf{s}_i \cdot \mathbf{l}_i + \alpha L(L+1) + \sum_k \left(F^k f_k + P^k p_k + T^k t_k + M^k m_k \right) \\ + \beta G(G_2) + \gamma G(R_7). \end{aligned} \tag{2}$$

Values of the parameters in (2) determined from simulations of the optical spectra are the following (in units of cm^{-1}): $F^2 = 96748$, $F^4 = 67943$, $F^6 = 55532$, $\zeta = 2368$, $\alpha = 18$, $\beta = -570$, $\gamma = 1631$, $P^2 = 653$, $P^4 = 326$, $P^6 = 65$, $M^0 = 3.6$, $M^2 = 0.56M_0$, $M^4 = 0.31M_0$, $T^2 = 451$, $T^3 = 61$, $T^4 = 100$, $T^6 = -245$, $T^7 = 305$, $T^8 = 160$ (conventional notations).

The Hamiltonian of the Yb^{3+} ion is considered in the framework of the model derived in Ref. [24] where we account for the hybridization of the 4f states of a hole at the Yb^{3+} ion with the charge transfer states of the complex containing the Yb^{3+} ion and two its nearest neighbor oxygen ions (namely, with the states of the holes at the 2p oxygen shells due to transfer of an electron from O^{2-} ions into the ytterbium $4f^{13}$ shell).

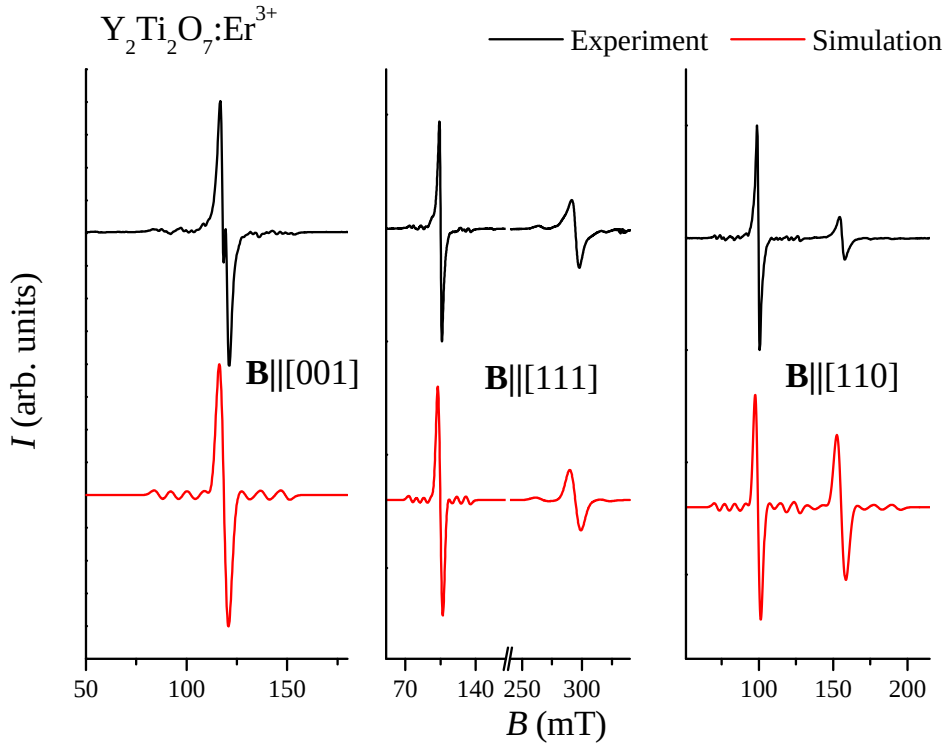

Figure 4. EPR spectra of the $Y_2Ti_2O_7$:Er^{3+} (0.5 at.%) single-crystal for three orientations of the magnetic field **B** ($\nu = 9.41553$ GHz, $T = 20$ K). Experimental data and the results of simulations are shown by solid black and red lines, respectively. Linewidths of the spectral components of the simulated spectra had the values of $\sigma = 0.18$ GHz for $\mathbf{B} \parallel [001]$ and $\mathbf{B} \parallel [110]$, and $\sigma_1 = 0.15$ GHz and $\sigma_2 = \sigma_3 = \sigma_4 = 0.225$ GHz for $\mathbf{B} \parallel [111]$.

The local systems of coordinates defined in [30] for RE ions at sites with the radius-vectors $\mathbf{r}_n$ are used in calculations: the Z_n axes are parallel to $\mathbf{r}_n$ and the X_n axes are in the planes containing $\mathbf{r}_n$ and the selected crystallographic tetragonal axis coinciding with the z-axis of the global coordinate frame. The CF Hamiltonian written in the local system of coordinates,

$$H_{\rm CF} = \sum (B_2^0 O_2^0 + B_4^0 O_4^0 + B_4^3 O_4^3 + B_6^0 O_6^0 + B_6^3 O_6^3 + B_6^6 O_6^6), \qquad (3)$$

determined by six non-zero CF parameters B_p^k (here O_p^k are linear combinations of the single-electron spherical tensor operators [22]), the sum is taken over 4f electrons with radius vectors **r**, orbital and spin moments **l** and **s**, respectively. The values of the CF parameters used to simulate the EPR spectra, the dc-susceptibility and the magnetization data are given in Table 1. The operator corresponding to the Zeeman energy has the form of $H_{\rm Z} = -\boldsymbol{\mu} \cdot \mathbf{B}$, where $\boldsymbol{\mu} = -\mu_{\rm B}(k\mathbf{L} + 2\mathbf{S})$ is the magnetic moment of a RE ion, **L** and **S** are orbital and spin moments, respectively, and k is the orbital reduction factor ($k = 0.99$ for the Er^{3+} ion and 0.98 for the Yb^{3+} ion).

Table 1. CF parameters B_p^k (cm^{-1}) for the impurity RE^{3+} ions in $Y_2Ti_2O_7$:Er^{3+} and $Y_2Ti_2O_7$:Yb^{3+}.

pk	20	40	43	60	63	66
Er^{3+}	239.8	311.8	−2305.2	45.7	666.6	753.2
Yb^{3+}	264.8	270.8	−2155.2	44.9	636.6	683.2

The Hamiltonian of hyperfine interactions H_{HF} contains magnetic H_{HFM} and quadrupole H_{HFQ} contributions:

$$\begin{aligned} H_{\mathrm{HFM}} = \mu_{\mathrm{B}}\gamma_{\mathrm{N}}\hbar\left\langle r^{-3}\right\rangle_{4\mathrm{f}} \sum \{2\mathbf{I}\cdot\mathbf{l} + O_2^0\left(3s_zI_z - \mathbf{s}\cdot\mathbf{I}\right) + 3O_2^2\left(s_xI_x - s_yI_y\right) \\ + 3O_2^{-2}\left(s_xI_y + s_yI_x\right) + 6O_2^1\left(s_zI_x + s_xI_z\right) + 6O_2^{-1}\left(s_yI_z + s_zI_y\right)\}, \end{aligned} \tag{4}$$

$$\begin{aligned} H_{\mathrm{HFQ}} = \frac{e^2Q}{4I\left(2I-1\right)}\{(1-\gamma_\infty)\sum_L q_L\frac{3z_L^2 - r_L^2}{r_L^5}\left(3I_z^2 - I(I+1)\right) \\ - (1-R_Q)\left\langle r^{-3}\right\rangle_{4\mathrm{f}}\sum\left[O_2^0\left(3I_z^2 - I(I+1)\right) + 3O_2^2\left(I_x^2 - I_y^2\right)\right. \\ \left. + 3O_2^{-2}\left(I_xI_y + I_yI_x\right) + 6O_2^1\left(I_zI_x + I_xI_z\right) + 6O_2^{-1}\left(I_yI_z + I_zI_y\right)\right]\}. \end{aligned} \tag{5}$$

Here γ_{N} is the nuclear gyromagnetic ratio ($\gamma_{\mathrm{N}}/2\pi = -1.18$, 6.9 and $-1.98\,\mathrm{MHz/T}$ for ^{167}Er, ^{171}Yb and ^{173}Yb [31] respectively), $\left\langle r^{-3}\right\rangle_{4\mathrm{f}}$ is the expectation value of the r^{-3} operator over a 4f-electron radial wave function equal to 11.07 and 12.5 at. units for Er^{3+} and Yb^{3+} [32], respectively, Q is the quadrupole moment of the nucleus (Q =5.88 and 1.35 in units of $10^{-28}\,\mathrm{m}^2$ for ^{167}Er and ^{173}Yb [31], respectively), $\gamma_\infty = -80$ and $R_Q = 0.1$ are Sternheimer antishielding and shielding factors [33], $\hbar$ is the Planck constant. The first term in Eq. (5) comes from the crystal lattice contribution to the electric field gradient at the nucleus and contains the sum over the host lattice ions with charges q_L and radius vectors $\mathbf{r}_L$ relative to the considered RE ion.

The CF energies of RE ions were found by numerical diagonalization of the operator $H_0 = H_{\mathrm{FI}} + H_{\mathrm{CF}}$. The matrices of the operators H_{Z} and H_{HF} were computed in the space of eigenfunctions of H_0, and the subsequent calculations were carried out with the Hamiltonian $H = E_0 + H_{\mathrm{Z}} + H_{\mathrm{HF}}$ (here E_0 is the diagonal matrix with elements equal to eigenvalues of H_0).

The average values of magnetic moments of RE ions versus the magnetic field B and temperature T were computed in the local systems of coordinates accordingly to the definition

$$\langle\boldsymbol{\mu}\rangle_{\mathbf{B},T} = \frac{\mathrm{Tr}\left[\boldsymbol{\mu}\exp\left(-(E_0 - \boldsymbol{\mu}\cdot\mathbf{B})/k_{\mathrm{B}}T\right)\right]}{\mathrm{Tr}\left[\exp(-(E_0 - \boldsymbol{\mu}\cdot\mathbf{B})/k_{\mathrm{B}}T)\right]} \tag{6}$$

The obtained field dependences of the magnetization

$$M(\mathbf{B},T) = \frac{cN_{\mathrm{A}}}{4B}\sum_{n=1}^{4}\mathbf{B}\cdot\langle\boldsymbol{\mu}_n\rangle_{\mathbf{B},T}, \tag{7}$$

where the sum is taken over four nonequivalent RE sites in the unit cell, are compared with the experimental data in Figure 2. The magnetic susceptibility tensor in the local system of coordinates is diagonal and has only two different components $\chi_\perp = \chi_{XX} = \chi_{YY}$, $\chi_\parallel = \chi_{ZZ}$. The computed temperature dependences of the isotropic bulk magnetic susceptibilities $\chi(T) = [\chi_\parallel(T) + 2\chi_\perp(T)]/3$ of $Y_2Ti_2O_7$:Er^{3+} and $Y_2Ti_2O_7$:Yb^{3+} are compared with the results of measurements in Figure 2.

The EPR spectra corresponding to magnetic dipole transitions between sublevels of the well isolated ground doublet split by the external magnetic field can be described by the spin-Hamiltonian H_{S} which represents the projection of the total Hamiltonian H of an ion on the 2-dimensional ground state manifold. In the local system of coordinates, the spin-Hamiltonian is written as follows (we neglect nuclear Zeeman and quadrupole energies)

$$H_{\mathrm{S}} = g_\parallel\mu_{\mathrm{B}}B_zS_z + g_\perp\mu_{\mathrm{B}}\left(B_xS_x + B_yS_y\right) + A_\parallel I_zS_z + A_\perp\left(I_xS_x + I_yS_y\right), \tag{8}$$

Table 2. The spin-Hamiltonian parameters for impurity Yb^{3+} and Er^{3+} ions in $Y_2Ti_2O_7$ (the signs of the hyperfine constants are obtained from theoretical analysis).

	^{171}Yb	^{171}Yb	^{173}Yb	^{173}Yb	^{167}Er	^{167}Er
	Exper.	Theory	Exper.	Theory	Exper.	Theory
$g_\parallel$	1.787	1.864	1.787	1.864	2.29	2.305
$g_\perp$	4.216	4.181	4.216	4.181	6.76	6.811
$A_\parallel$ (MHz)	1235	1353	−353.8	−388	−277.4	−252
$A_\perp$ (MHz)	3064	3050	−881.4	−875	−810.9	−735

where the effective spin $S = 1/2$, $g_\parallel$ and $g_\perp$ are components of the g-tensor, $A_\parallel$ and $A_\perp$ are the magnetic hyperfine constants. Exactly these spin-Hamiltonian parameters were determined from the analysis of the measured EPR spectra (see Table 2, columns "Exper.").

The magnetic hyperfine interaction (4) can be written as follows: $H_{\rm HFM} = \mathbf{a} \cdot \mathbf{I}$, here the components of the vector $\mathbf{a}$

$$a_x = \mu_{\rm B}\gamma_{\rm N}\hbar\langle r^{-3}\rangle_{\rm 4f} \sum \left[2l_x - (O_2^0 - 3O_2^2)s_x + 3O_2^{-2}s_y + 6O_2^1 s_z\right], \tag{9}$$

$$a_y = \mu_{\rm B}\gamma_{\rm N}\hbar\langle r^{-3}\rangle_{\rm 4f} \sum \left[2l_y - (O_2^0 + 3O_2^2)s_y + 3O_2^{-2}s_x + 6O_2^{-1} s_z\right], \tag{10}$$

$$a_z = 2\mu_{\rm B}\gamma_{\rm N}\hbar\langle r^{-3}\rangle_{\rm 4f} \sum \left[l_z + O_2^0 s_z + 3O_2^1 s_x + 3O_2^{-1} s_y\right] \tag{11}$$

operate in the space of electronic wave functions. The components of the g-tensor and the hyperfine constants in the spin-Hamiltonian are calculated using the expressions

$$g_\parallel = 2\langle +| kL_z + 2S_z |+\rangle, \quad g_\perp = 2\langle +| kL_x + 2S_x |-\rangle, \tag{12}$$

$$A_{||} = 2\langle +| a_z |+\rangle, \quad A_\perp = 2\langle +| a_x |-\rangle, \tag{13}$$

where $|+\rangle$ and $|-\rangle$ are the eigenfunctions of the Hamiltonian H_0 corresponding to the ground CF doublet of a Kramers ion. The equations (12), (13) pave a bridge between the spin-Hamiltonian and crystal-field approaches. The calculated parameters of the spin-Hamiltonian (Table 2, columns "Theory") agree with the experimental data. We note that the obtained values of g-factors for Yb^{3+} ions are close to those communicated in Ref. [15] ($g_\parallel$=1.79, $g_\perp$=4.27) for $^{170}Yb^{3+}$ ions in the sample of $Y_2Ti_2O_7$:Yb^{3+} (1 at.%). The estimated shifts of the hyperfine sublevels of the ground doublets of the $^{167}Er^{3+}$ and $^{173}Yb^{3+}$ ions induced by the quadrupole hyperfine interaction (5) which are less than 250 MHz, were not revealed in the measured spectra.

The relative integral intensities W_{ij} of the resonant magnetic dipole transitions $i \to j$ between the eigenstates of the spin-Hamiltonian (8) with energies E_i, E_j and wave functions $|i\rangle$ and $|j\rangle$ induced by the microwave magnetic field $\mathbf{B}_1$ directed along the unit vector $\mathbf{e}$ perpendicular to the constant field $\mathbf{B}$ can be written as

$$W_{ij} = \left|\langle i|(g_\perp S_x e_x + g_\perp S_y e_y + g_\parallel S_z e_z)|j\rangle\right|^2. \tag{14}$$

The spectral distribution of absorption intensities for the fixed microwave frequency ν in the magnetic field $\mathbf{B}$ is approximated by the sum of Gaussians with the varied linewidth σ

$$I(B) \sim \sum_{ij} W_{ij}(p_i - p_j)\frac{1}{\sqrt{2\pi}\sigma}\exp[-(\Delta_{ji} - 2\pi\hbar\nu)^2/2\sigma^2], \tag{15}$$

here $\Delta_{ji} = E_j(\mathbf{B}) - E_i(\mathbf{B})$, $p_i(\mathbf{B})$ is the population of the state $|i\rangle$, and the sum over i and j is taken over all electron-nuclear sublevels of the electronic doublet in case of odd isotopes. As shown in Figures 3 and 4, the simulated spectral envelopes $dI(B)/dB$ reproduce well the registered EPR signals at different orientations of the magnetic fields.

4. Summary

We carried out detailed experimental and theoretical studies of static and dynamic magnetic properties of impurity Er^{3+} and Yb^{3+} ions in $Y_2Ti_2O_7$ single crystals. The crystal field approach was used to interpret the measured magnetic field and temperature dependences of the magnetization and the characteristics of the EPR spectra. The sets of the CF parameters determined earlier from the analysis of the optical spectra [24] allowed us to reproduce successfully the values of resonance fields and relative intensities of EPR signals for different orientations of the applied field and the magnetic anisotropy induced by strong fields in cubic pyrochlores $Y_2Ti_2O_7$:Yb^{3+} and $Y_2Ti_2O_7$:Er^{3+} containing small concentrations of 0.5 at.% of RE ions. The shapes of EPR lines including the fine hyperfine structures due to odd ^{171}Yb, ^{173}Yb and ^{167}Er isotopes were successfully modeled and the corresponding linewidths and parameters of hyperfine interactions were determined from the fitting procedure.

The obtained new information on single-ion spectral and magnetic properties of diluted RE pyrochlores can be used to revise parameters of the anisotropic exchange interactions in $Er_2Ti_2O_7$ and $Yb_2Ti_2O_7$.

Acknowledgments

Financial support of the Russian Science Foundation under Grant N. 19-12-00244 is acknowledged.

References

1. Hallas A. M., Gaudet J., Gaulin B. D. *Ann. Rev. Condensed Matter Phys.* **9**, 105 (2018).

2. Rau J. G., Gingras M. J. P. *Annu. Rev. Condens. Matter Phys.* **10**, 357 (2019).

3. Yan H, Benton O., Jaubert L., Shannon N.*Phys. Rev. B* **95**, 094422 (2017).

4. Champion J. D. M., Harris M. J., Holdsworth P. C. W., Wills A. C., Balakrishnan G., Bramwell S. T., Cizmar E., Fennell T., Gardner J. S., Lago J., McMorrow D. F., Orendac M., Orendacova A., Paul D. McK., Smith R. J., Telling M. T. F., Wildes A. *Phys. Rev. B* **68**, 020401(R) (2003).

5. Poole A., Wills A. S., Lelievre-Berna E., Perring T. G., Dogan F. *J. Phys.: Condens. Matter* **19**, 452201 (2007).

6. Dun Z. L., Li X., Freitas R. S., Arrighi E., Dela Cruz C. R., Lee M., Choi E. S., Cao H. B., Silverstein H. J., Wiebe C. R., Cheng J. G., Zhou H. D. *Phys. Rev. B* **92**, 140407 (2015).

7. Hallas A. M., Gaudet J., Wilson M. N., Munsie T. J., Aczel A. A., Stone M. B., Freitas R. S., Arevalo-Lopez A. M., Attfield J. P., Tachibana M., Wiebe C. R., Luke G. M., Gaulin B. D. *Phys. Rev. B* **93**, 104405 (2016).

8. Petit S., Lhotel E., Damay F., Boutrouille P., Forget A., Colson D. *Phys. Rev. Lett.* **119**, 187202 (2017).

9. Hallas A. M., Gaudet J., Butch N. P., Xu G., Tachibana M., Wiebe C. R., Luke G. M., Gaulin B. D. *Phys. Rev. Lett.* **119**, 187201 (2017).

10. Yasui Y., Soda M., Iikubo S., Ito M., Sato M., Hamaguchi N., Matsushita T., Wada N., Takeuchi T., Aso N., Kakurai K. *J. Phys. Soc. Jpn.* **72**, 3014 (2003).

11. Chang L.-J., Onoda S., Su Y., Kao Y.-J., Tsuei K.-D., Yasui Y., Kakurai K., Lees M. R. *Nature Commun.* **3**, 992 (2012).

12. Yaouanc A., Dalmas de Reotier P., Bonville P., Hodges J. A., Glazkov V., Keller L., Sikolenko V., Bartkowiak M., Amato A., Baines C., King P. J. C., Gibbens P. C. M., Forget A. *Phys. Rev. Lett.* **110**, 127207 (2013).

13. Yasui Y., Hamachi N., Kono Y., Kittaka S., Sakakibara T. *SPIN* **5**, 1540002 (2015).

14. Yaouanc A., de Reotier P. D., Keller L., Roessli B., Forget A.*J. Phys.: Condens. Matter* **28**, 426002 (2016).

15. Hodges J. A., Bonville P., Forget A., Rams M., Królas K., Dhalenne G. *J. Phys.: Condens. Matter* **13**, 419301 (2001).

16. Cao H., Gukasov A., Mirebeau I., Bonville P., Decorse C., Dhalenne G. *Phys. Rev. Lett.* **103**, 056402 (2009).

17. Malkin B. Z., Zakirov A. R., Popova M. N., Klimin S. A., Chukalina E. P., Antic-Fidancev E., Goldner Ph., Aschehoug P., Dhalenne G. *Phys. Rev. B* **70**, 075112 (2004).

18. Gaudet J., Maharaj D. D., Sala G., Kermarrec E., Ross K. A., Dabkowska H. A., Kolesnikov A. I., Granroth G. E., Gaulin B. D. *Phys. Rev. B* **92**, 134420 (2015).

19. Sala G., Maharaj D. D., Stone M. B., Dabkowska H. A., Gaulin B. D. *Phys. Rev. B* **97**, 224409 (2018).

20. Gaudet J., Hallas A. M., Kolesnikov A. I., Gaulin B. D. *Phys. Rev. B* **97**, 024415 (2018).

21. Gardner J. S., Ehlers G. *J. Phys.: Conens. Matter* **21**, 436004 (2009).

22. Malkin B. Z., Lummen T. T. A., van Loosdrecht P. H. M., Dhalenne G., Zakirov A. R. *J. Phys.: Condensed Matter* **22**, 276003 (2010).

23. Bertin A., Chapuis Y., Dalmas de Réotier P., Yaouanc A. *J. Phys.: Conens. Matter* **24**, 256003 (2012).

24. Batulin R. G., Cherosov M. A., Gilmutdinov I. F., Khaliulin B. F., Kiiamov A. G., Klekovkina V. V., Malkin B. Z., Mukhamedshin I. R., Mumdzhi I. E., Nikitin S. I., Rodionov A. A., Yusupov R. V. *Physics of the Solid State* **61**, 818 (2019).

25. Li Q. J., Xu L. M., Fan C., Zhan F. B., Lv Y. Y., Ni B., Zhao Z. Y., Sun X. F. *J. Cryst. Growth* **377**, 96 (2013).

26. Bain G. A., Berry J. E. *J. Cryst. Growth* **85**, 532 (2008).

27. Cao H. B., Gukasov A., Mirebeau I., Bonville P., Decorse C., Dhalenne G. *Phys. Rev. Lett.* **103**, 056402 (2009).

28. Sosin S. S., Prozorova L. A., Lees M. R., Balakrishnan G., Petrenko O. A. *Phys. Rev. B* **82**, 094428 (2010).

29. Crosswhite H. M., Crosswhite H. *J. Opt. Soc. Am. B* **1**, 246 (1984).

30. Klekovkina V. V., Zakirov A. R., Malkin B. Z, Kasatkina L. A. *J. Phys.: Conf. Ser.* **324**, 012036 (2011).

31. McCausland M. A. H., Mackenzie I. S. *Adv. Phys.* **28**, 305 (1979).

32. Abragam A., Bleaney B. *Electron Paramagnetic Resonance of Transition Ions*, Clarendon Press, Oxford, UK (1970).

33. Gupta R. P., Sen S. K. *Phys. Rev. A* **7**, 850 (1973).